Quantifying Redundancy and Information Content of Lines in Recurrence Plots Using the Theory of Framework Rigidity

Aloys Sipers, Paul Borm and Ralf Peeters

Abstract We address redundancy in the information content of unthresholded recurrence plots (URPs). The theory of framework rigidity is employed to explain and analyze this redundancy geometrically. First we show that the domain of a URP can be restricted to just a finite number of vertical or horizontal lines without loss of information. Then we construct a globally rigid framework to demonstrate a similar property for diagonal lines. This result gives theoretical support to recurrence quantification analysis (RQA), which analyzes and extracts features from an RP along such lines. Third, we construct a finite set of curves, one of which is a contour line, for which it again holds that the URP contains all information along them. This links the information content of lossy (thresholded) recurrence plots to that of URPs. This study is also a starting point in employing redundancy to improve existing recurrence plots based methods and algorithms, and to develop new ones. Several examples clarify the methods and an application from EEG artifact detection shows some of their practical potential.

1 Introduction

Recurrence plots (RPs), see [1], are a popular tool for the visualization of the behavior of dynamical systems, in particular for their phase space trajectories. Recurrence quantification analysis (RQA), see [2, 3], provides RP based methods to further

A. Sipers (✉) · P. Borm
Centre of Expertise in Life Sciences, Zuyd University,
Nieuw Eyckholt 300, 6419 DJ Heerlen,
The Netherlands
e-mail: aloys.sipers@zuyd.nl

P. Borm
e-mail: paul.borm@zuyd.nl

R. Peeters
Department of Knowledge Engineering, Universiteit Maastricht,
Bouillonstraat 8-10, 6200 MD
Maastricht, The Netherlands
e-mail: ralf.peeters@maastrichtuniversity.nl

N. Marwan et al. (eds.), *Translational Recurrences*, Springer Proceedings
in Mathematics & Statistics 103, DOI 10.1007/978-3-319-09531-8_4

analyze and quantify RPs and the underlying dynamical behavior. RQA proceeds by selecting horizontal, vertical and diagonal lines in recurrence plots and computing various quantities from them. Potential problems and pitfalls related to different aspects of the application of RPs are pointed out in [4]. The methods based on RPs have been successfully applied to various fields in the natural sciences as well as in engineering and in economy. See, for instance, the bibliography collected on the recurrence plot website [5], which shows an impressive increase of such applications over the last decade.

Recurrence plots can also be used to analyze scalar signals $x(t)$ by first embedding them in an M-dimensional trajectory space. Given a finite-interval continuous-time real-valued signal $x(t)$, with $t \in [0, 1)$ say, the time-delay embedding method of [6] constructs such a trajectory $X(t)$ as:

$$X(t) = \begin{pmatrix} x(t) \\ x(t+\tau) \\ \vdots \\ x(t+(M-1)\tau) \end{pmatrix}, \qquad t \in [0, 1). \tag{1}$$

The embedding dimension M and the time-delay $\tau \in (0, 1)$ are specified by the user, for which some techniques are available in the literature, e.g. involving the average mutual information (AMI) [7] for M, or the false nearest neighbors fraction (FNNF) [8] for τ. Next, the *unthresholded* recurrence plot (URP) is defined as (the graph of) the intra-trajectory distance function for $X(t)$:

$$\mathrm{URP}_X(u, v) = \|X(u) - X(v)\|, \qquad u, v \in [0, 1), \tag{2}$$

in which $\|\cdot\|$ denotes a norm. While several other norms are also popular in the literature, such as the 1-norm and the maximum norm, we will exclusively use the Euclidean norm here. Also, to avoid having to take finite interval effects explicitly into account, the signal $x(t)$ and its trajectory $X(t)$ are periodically extended from the interval $[0, 1)$ to all of $\mathbb{R}$. Finally, for a given positive threshold ε, the *binary* (thresholded) recurrence plot is defined as

$$\mathrm{RP}^{\varepsilon}_X(u, v) = \Theta\left(\varepsilon - \|X(u) - X(v)\|\right), \qquad u, v \in [0, 1), \tag{3}$$

in which Θ denotes the Heaviside function (i.e. $\Theta(x) = 1$ for $x \geq 0$ and $\Theta(x) = 0$ otherwise). Recurrence plots can likewise be defined for discrete-time signals and trajectories in an obvious way, by restricting t, u and v to a discrete set of time instants (and choosing τ accordingly).

For a proper understanding of the information content of a recurrence plot, we have previously addressed the relationship between the URP and its underlying signal $x(t)$ using Fourier analysis and graph theory; see [9]. Generically it holds that URP_X determines $x(t)$ up to a sign and an additive constant, but more information from $x(t)$ may sometimes be lost, depending on the frequency content of $x(t)$ and

on the choice of the embedding parameters M and τ. Earlier work in this area is found in [10, 11], while the relationship between the RP and $x(t)$ was previously investigated in [12–15]. In the present paper we study redundancy of information in URPs themselves. One obvious aspect of URPs and RPs is their symmetry with respect to the diagonal $u = v$. Since URPs are a 2-dimensional representation of a 1-dimensional object (the trajectory in M-dimensional space), it should also not come as a surprise that it carries much more redundant information. We first address the joint information content of horizontal and vertical lines in a URP and we show how this determines the (redundant) information in other parts of that URP. As an example, we show how our results on redundancy in URPs can be employed for the detection of similar signal segments. (Other detection methods based on RPs can also be found in [16–18].) For further studies on lines structures in RPs, see e.g. [2, 19, 20]. We shall also briefly address the information in diagonals and in contour lines of a URP. This aims to better understand the information which is preserved in an RP, as an RP is obtained from a URP by thresholding.

Because a URP captures distance information between pairs of points on the trajectory $X(t)$, it is natural to employ the theory of framework rigidity, see [21–23], to explain geometrically the redundant distance information in a URP. Following [23], we introduce some preliminary definitions and notation. A *configuration* P in $\mathbb{R}^M$ is a finite set of N points $P = \{P_1, P_2, \ldots, P_N\}$. Let G be a simple graph on the nodes $1, 2, \ldots, N$, then a *bar-and-joint framework* (or simply a *framework*) in $\mathbb{R}^M$, denoted by $G(P)$, is the graph G together with the configuration P, where each node n of G is located at the point P_n. Each edge (m, n) in G is viewed as a rigid bar of length equal to $\|P_m - P_n\|$, and each node in G as a joint – with full rotational freedom for all its adjacent bars. Two frameworks $G(P)$ and $G(Q)$ are said to be *equivalent* if $\|P_m - P_n\| = \|Q_m - Q_n\|$ for all edges (m, n) of G. They are said to be *congruent* if $\|P_m - P_n\| = \|Q_m - Q_n\|$ for all pairs of nodes m and n in the graph G. This is the same as saying that $G(Q)$ can be obtained from $G(P)$ by an isometry. A framework $G(P)$ is called *rigid* if there is an $\epsilon > 0$ such that every framework $G(Q)$ which is equivalent to $G(P)$ and for which $\|P_n - Q_n\| < \epsilon$ for all $n = 1, 2, \ldots, N$, is also congruent to $G(P)$. A framework is called *globally rigid* if this holds for every $\epsilon > 0$, i.e. if every framework $G(Q)$ which is equivalent to $G(P)$ is congruent to $G(P)$. A complete graph always gives a globally rigid framework for every embedding dimension M. See Fig. 1 for an example of four frameworks in $\mathbb{R}^2$ illustrating these concepts, where the nodes (joints) are represented by dots and the edges (bars) by straight lines.

In this paper we consider frameworks $G(\mathcal{X})$ which involve a configuration of points $\mathcal{X} = \{\mathcal{X}_1, \ldots, \mathcal{X}_N\}$ located on a trajectory $X(t)$. i.e. for all nodes $n = 1, \ldots, N$ of G: $\mathcal{X}_n = X(t_n)$ for some set of time instants $t_1, \ldots, t_N$. Note that global rigidity of $G(\mathcal{X})$ then expresses the property that all the values of $\mathrm{URP}_X(u, v)$ with $u, v \in \{t_1, \ldots, t_N\}$ are determined by the subset of such values with (u, v) corresponding to the edges of G.

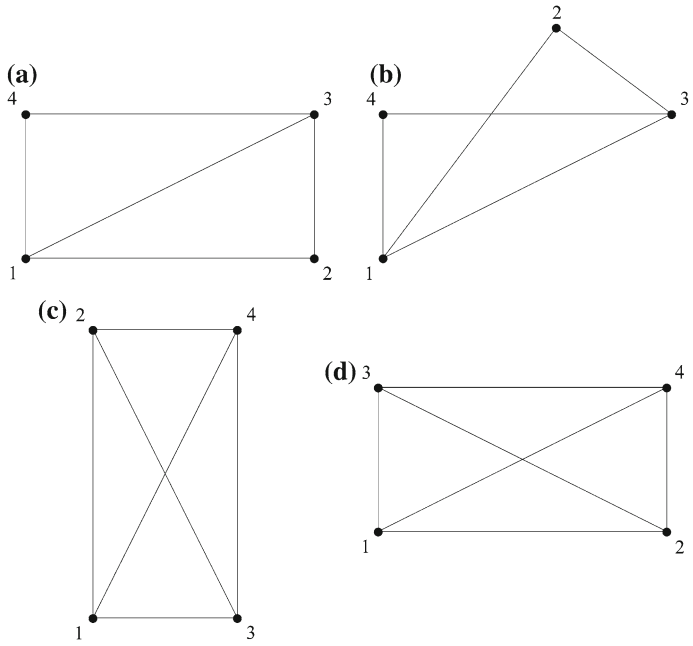

Fig. 1 The frameworks in **a** and **b** are equivalent. When embedded in $\mathbb{R}^2$, both are rigid. They are not congruent, therefore they are both not globally rigid. When embedded in $\mathbb{R}^3$ they are both also no longer rigid. The frameworks in **c** and **d** are congruent and both are globally rigid. The graph G is complete; therefore global rigidity holds for arbitrary embedding dimensions ≥ 2

The paper is structured as follows. In Sect. 2, we show that the whole URP can be reconstructed from the information content of a set of selected horizontal or vertical lines in a URP. The geometrical interpretation and the use of redundancy in recurrence plot analysis is demonstrated and evaluated by three examples. First, redundant distance information in a trajectory and in its URP is illustrated geometrically. Second, we show that the choice of the embedding parameters M and τ may influence the number of lines needed in the URP to capture all the information. Third, an application in EEG analysis involving eye blink artifact detection is presented, to demonstrate how redundancy can be employed to reduce the analysis region for the URP. In Sect. 3, we construct globally rigid frameworks with points which relate to diagonals of a URP, and then we extend that approach to (approximate) contour lines. This aims to better understand the information which is (and which is not) preserved in RPs. Section 4 concludes the paper. All the proofs are collected in the Appendix.

2 Redundancy in URPs and the Information Contained in Vertical Lines

In this section we show with basic geometry how an entire URP can be reconstructed from the information it carries in a few well selected horizontal or vertical lines. Because URP_X is constructed from the intra-trajectory distances of $X(t)$ in the embedding space $\mathbb{R}^M$, it is clear that it is invariant under isometric transformation of $X(t)$, which makes it natural to employ affine geometric tools. To formalize this we have the following basic results.

Lemma 1 *Let V_X be the smallest affine subspace of $\mathbb{R}^M$ which contains the trajectory $X(t)$. Denote $k = dim(V_X)$. Let $\mathbb{T}_b = \{t_0, t_1, \ldots, t_k\}$ be a set of time instants such that $\{X(t_0), X(t_1), \ldots, X(t_k)\}$ constitutes an affine basis for V_X. Each point $X(t)$ can then be written in a unique way as $X(t) = \sum_{m=0}^{k} \alpha_m(t) X(t_m)$ with affine coordinates $\alpha_m(t) \in \mathbb{R}$, satisfying $\sum_{m=0}^{k} \alpha_m(t) = 1$.*
Relative to the point $X(t_0)$, let the trajectory be represented by $\widetilde{X}(t) := X(t) - X(t_0)$, so that a basis for the linear space $V_X - X(t_0)$ is given by the columns of the matrix $B := \left(\widetilde{X}(t_1)\middle|\ldots\middle|\widetilde{X}(t_k)\right)$. Note that for this basis, the coordinate vector of $\widetilde{X}(t)$ is the unique vector $\alpha(t)$ satisfying $\widetilde{X}(t) = B\alpha(t)$. Its entries coincide with the affine coordinates: $\alpha(t) = (\alpha_1(t), \ldots, \alpha_k(t))^T$. We then have that:

(1) The coordinate vector $\alpha(t)$ of $\widetilde{X}(t)$ is given by

$$\alpha(t) = (B^T B)^{-1} B^T \widetilde{X}(t). \tag{4}$$

(2) The values $URP_X(u, v)$ of the unthresholded recurrence plot satisfy:

$$URP_X(u, v)^2 = (A(u) - A(v))^T \left(B^T B\right)^{-1} (A(u) - A(v)), \tag{5}$$

where

$$A(t) := B^T \widetilde{X}(t) = B^T B\alpha(t). \tag{6}$$

(3) For $m = 1, \ldots, k$, the entries $A_m(t)$ of $A(t)$ are given in terms of URP_X by:

$$A_m(t) = \frac{1}{2}\left(URP_X(t_0, t_m)^2 + URP_X(t_0, t)^2 - URP_X(t_m, t)^2\right). \tag{7}$$

(4) For $m, n = 1, \ldots, k$, the entries $\left(B^T B\right)_{m,n}$ of the Gram matrix $B^T B$ are given by:

$$\left(B^T B\right)_{m,n} = A_m(t_n) = A_n(t_m). \tag{8}$$

Combining parts (2), (3) and (4) of this lemma, it follows that $\mathrm{URP}_X(u, v)$ can be computed from the joint information stored at certain other locations in the URP. We have the following theorem.

Theorem 1 *Let V_X be the smallest affine subspace of $\mathbb{R}^M$ containing the trajectory $X(t)$. Denote $k = dim(V_X)$. Let $\mathbb{T}_b := \{t_0, t_1, \ldots, t_k\}$ be a set of time instants such that $\{X(t_0), X(t_1), \ldots, X(t_k)\}$ is an affine basis for V_X. Then:*
(1) The entire unthresholded recurrence plot $URP_X(u, v)$ can be computed from the restriction of $URP_X(u, v)$ to the $k + 1$ vertical lines of points (u, v) with $u \in \mathbb{T}_b$.
(2) Let $\mathbb{T}_a \subseteq [0, 1)$ be an arbitrary subset of time instants. Then the restriction of $URP_X(u, v)$ to $\mathbb{T}_a \times \mathbb{T}_a$ can be computed from the restriction of $URP_X(u, v)$ to $\mathbb{T}_b \times (\mathbb{T}_b \cup \mathbb{T}_a)$.

According to part (1) of this theorem, the dimension k of the affine subspace V_X determines how many vertical lines jointly carry all the information in a URP. (By symmetry, this likewise holds for horizontal lines.) The value of k is bounded from above by the embedding dimension M, but it may also vary with the choice of time-delay τ. We can make this precise for time-delay embeddings of real periodic signals $x(t)$ which have a Fourier series representation $x(t) = \sum_{p\in\mathbb{Z}} c_p e^{2\pi pti}$. For such signals it holds that the complex Fourier coefficients c_p satisfy $c_{-p} = \overline{c_p}$ for all $p \in \mathbb{Z}$. The corresponding trajectory $X(t)$ is given by $X(t) = \sum_{p\in\mathbb{Z}} c_p e^{2\pi pti} T_p$, in which the complex-valued vectors $T_p \in \mathbb{C}^M$ are given by:

$$T_p = \begin{pmatrix} 1 \\ z^p \\ \vdots \\ z^{(M-1)p} \end{pmatrix}, \qquad \text{with } z = e^{2\pi\tau i}. \tag{9}$$

See also [9], where this class was used extensively. We then have the following result.

Proposition 1 *Let $x(t)$ be a real periodic signal with a Fourier series representation $x(t) = \sum_{p\in\mathbb{Z}} c_p e^{2\pi pti}$. Let k be the dimension of the smallest affine subspace V_X of $\mathbb{R}^M$ containing the trajectory $X(t) = \sum_{p\in\mathbb{Z}} c_p e^{2\pi pti} T_p$. Define the set $K_X := \{p \in \mathbb{Z} \setminus \{0\} \mid c_p \neq 0\}$ and define the linear subspace $\mathcal{V}$ of $\mathbb{C}^M$ as the span of the set of vectors T_p with $p \in K_X$. Then:*
(1) $k = dim(\mathcal{V})$.
(2) Let r be the cardinality of the set $\{p\tau (mod\ 1) \mid p \in K_X\}$, i.e. the total number of different fractional parts of the quantities $p\tau$ with $p \in K_X$. Then $k = \min\{M, r\}$.

For values of τ that are not rational, all the quantities $p\tau \pmod 1$ with $p \in K_X$ are different. Then part (2) of this proposition shows that $k = \min\{M, |K_X|\}$ and the dimension k of V_X attains its maximal value (i.e. for the situation where τ is varied but M and the signal $x(t)$ are fixed). Because the vectors T_p all depend continuously on τ, it follows from part (1) that the same maximal value of k is also attained in open neighborhoods of such irrational values for τ and hence it is attained generically. However, for some special rational choices of τ (e.g. in combination with finite sets K_X), the value of k may drop.

To further clarify the findings of this section, we now give three examples. In the first example we explain geometrically the redundant distance information contained in a URP. In the second example we investigate the impact of different choices of τ, which may lead to different values of the dimension $k = \dim(V_X)$. In the third example we investigate an application in EEG analysis. It concerns a digitally sampled measurement signal containing eye blink artifacts. We demonstrate how the set of time instants $\mathbb{T}_b$ in Theorem 1 can be chosen to reduce the analysis region from the entire URP to only a part.

Example 1 Parts of a URP constructed from vertical lines in that URP

To illustrate Theorem 1 and the underlying Lemma 1, we consider a trajectory $X(t)$ in $\mathbb{R}^2$ and a set of time instants $\mathbb{T}_b = \{t_0, t_1, t_2\}$, for three different choices of $\mathbb{T}_a$.
(i) Let $\mathbb{T}_a = \{u_0, v_0\}$.
From Lemma 1 we have that $\mathrm{URP}_X(u_0, v_0)$ is determined by the entries of $A(u_0)$, $A(v_0)$ and $B^T B$. The entries of $B^T B$ are in turn given by the entries of $A(t_1)$ and $A(t_2)$. The entries of a vector $A(t)$ are determined by $\mathrm{URP}_X(t_0, t)$, $\mathrm{URP}_X(t_1, t)$, $\mathrm{URP}_X(t_2, t)$, $\mathrm{URP}_X(t_0, t_1)$ and $\mathrm{URP}_X(t_0, t_2)$. With $t \in \{t_1, t_2, u_0, v_0\}$, it therefore follows that $\mathrm{URP}_X(u_0, v_0)$ is determined by:

(1) The values $\mathrm{URP}_X(t_0, t_1)$, $\mathrm{URP}_X(t_0, t_2)$ and $\mathrm{URP}_X(t_1, t_2)$, which equal the lengths of the three black solid lines in Fig. 2a. Note that this constitutes the complete graph for the affine basis of trajectory points $\{X(t_0), X(t_1), X(t_2)\}$ for $\mathbb{T}_b$.
(2) The values $\mathrm{URP}_X(t_0, u_0)$, $\mathrm{URP}_X(t_1, u_0)$ and $\mathrm{URP}_X(t_2, u_0)$, which equal the lengths of the three red solid lines in Fig. 2a. These values fix the position of the point $X(u_0)$ relative to the affine basis under (1).
(3) The values $\mathrm{URP}_X(t_0, v_0)$, $\mathrm{URP}_X(t_1, v_0)$ and $\mathrm{URP}_X(t_2, v_0)$, which equal the lengths of the three green solid lines in Fig. 2a. These values fix the position of the point $X(v_0)$ relative to the affine basis under (1).

The key geometric observation is that the framework $G(P)$ with P consisting of the trajectory points for the time instants $\mathbb{T}_a \cup \mathbb{T}_b$ and which has all the possible edges except for the edge between $X(u_0)$ and $X(v_0)$ (represented by the blue dashed line in Fig. 2a), is a *globally rigid* framework. Therefore the value of $\mathrm{URP}_X(u_0, v_0)$ is fixed. In Fig. 2b, the corresponding points in the recurrence plot URP_X are indicated: the blue dot for (u_0, v_0), three black dots for (t_0, t_1), (t_0, t_1), (t_1, t_2), three red dots for (t_0, u_0), (t_1, u_0), (t_2, u_0), and three green dots for (t_0, v_0), (t_1, v_0), (t_2, v_0). Because of symmetry, and because the values of any URP along the diagonal $u = v$ are all zero, the statements of Theorem 1 follow (also for horizontal lines).
(ii) Let $\mathbb{T}_a = [\alpha, \beta]$ be a subinterval of $[0, 1]$.
The restriction of $\mathrm{URP}_X(u, v)$ to the grid points $\mathbb{T}_b \times \mathbb{T}_b$ again corresponds to the complete graph for the affine basis of points $X(t_0)$, $X(t_1)$ and $X(t_2)$, previously indicated by the solid black triangle in Fig. 2a. The restriction of $\mathrm{URP}_X(u, v)$ to the

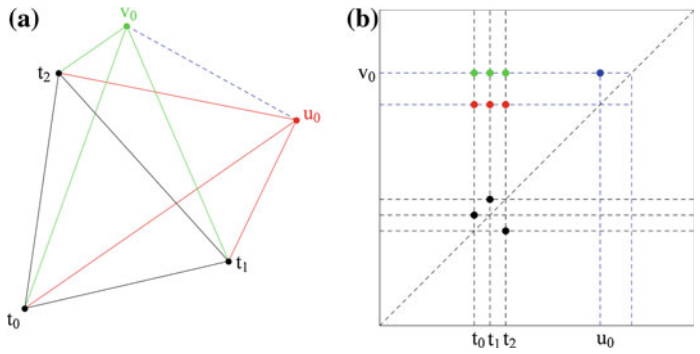

Fig. 2 Geometric representation of redundant distance information: **a** in a trajectory; **b** in its URP

three vertical line segments with coordinates in $\mathbb{T}_b \times [\alpha, \beta]$, captures the distances between the points $X(t)$ with $t \in [\alpha, \beta]$ and the three points of the affine basis; it fixes the position of these points $X(t)$ relative to the basis. Taking $u_0, v_0 \in [\alpha, \beta]$, the restriction of $\mathrm{URP}_X(u, v)$ to the square area $[\alpha, \beta] \times [\alpha, \beta]$ can then be constructed in a point-by-point manner as described under (i).
(iii) Suppose $\mathbb{T}_a = [0, 1]$. This is case (ii) for the special choice $\alpha = 0$ and $\beta = 1$. Then from the restriction of $\mathrm{URP}_X(u, v)$ to the three vertical lines with (u, v) in $\{t_0, t_1, t_2\} \times [0, 1]$, see Fig. 2b, all of $\mathrm{URP}_X(u, v)$ can be constructed.

Example 2 Influence of the embedding parameters M and τ on redundancy

Consider a zero-mean real-valued signal of the form $x(t) = \sum_{p=-2}^{2} c_p e^{2\pi p t i}$ with $c_{-p} = \overline{c_p} \neq 0$ for $p \in K_X = \{-2, -1, 1, 2\}$ and $c_0 = 0$. Let the embedding dimension be chosen as $M = 4$. The corresponding trajectory $X(t)$ is contained in a smallest affine subspace V_X of $\mathbb{R}^4$, which is in fact a linear subspace because of the zero-mean property. It therefore coincides with the intersection of $\mathbb{R}^4$ and the space $\mathcal{V}$ spanned by the four vectors $T_p \in \mathbb{C}^4$ with $p \in K_X$. According to Proposition 1(1) we have that: $k = \dim(V_X) = \dim(\mathcal{V}) = \mathrm{rank}\left(T_{-2} \middle| T_{-1} \middle| T_1 \middle| T_2\right)$. The latter matrix is a Vandermonde matrix for the 4 complex numbers in the set $\{\overline{z}^2, \overline{z}, z, z^2\}$ with $z = e^{2\pi\tau i}$. These are numbers on the complex unit circle and depend on τ. To find the value of k we must count how many different values are contained in this set. From Proposition 1(2) (and since $M = 4$) we have that k also equals the cardinality r of $\{p\tau \,(\mathrm{mod}\, 1) \mid p \in K_X\}$. We compute k for four different rational values of τ.

(1) $\tau = \frac{1}{2}$. Then $z = e^{\pi i} = -1$ and $|\{\overline{z}^2, \overline{z}, z, z^2\}| = |\{-1, 1\}| = 2$. Alternatively, $r = |\{p\tau \,(\mathrm{mod}\, 1) \mid p \in K_X\}| = |\{0, \frac{1}{2}\}| = 2$. Both approaches give $k = 2$.
(2) $\tau = \frac{1}{3}$. Now $z = e^{2\pi i/3}$ and $|\{\overline{z}^2, \overline{z}, z, z^2\}| = |\{e^{2\pi i/3}, e^{4\pi i/3}\}| = 2$. Also, $r = |\{p\tau \,(\mathrm{mod}\, 1) \mid p \in K_X\}| = |\{\frac{1}{3}, \frac{2}{3}\}| = 2$. It again follows that $k = 2$.

(3) $\tau = \frac{1}{4}$. Here $z = e^{\pi i/2} = i$ and $|\{\overline{z}^2, \overline{z}, z, z^2\}| = |\{i, -1, -i\}| = 3$. Likewise, $r = |\{p\tau \,(\mathrm{mod}\, 1) \mid p \in K_X\}| = |\{\frac{1}{4}, \frac{1}{2}, \frac{3}{4}\}| = 3$, whence $k = 3$.

(4) $\tau = \frac{1}{5}$. In this case $z = e^{2\pi i/5}$ and $|\{\overline{z}^2, \overline{z}, z, z^2\}| = |\{e^{2\pi i/5}, e^{4\pi i/5}, e^{6\pi i/5}, e^{8\pi i/5}\}| = 4$. Similarly, $r = |\{p\tau \,(\mathrm{mod}\, 1) \mid p \in K_X\}| = |\{\frac{1}{5}, \frac{2}{5}, \frac{3}{5}, \frac{4}{5}\}| = 4$. Now k attains its maximal possible value (for the given choice of M and $x(t)$): $k = 4$.

This example shows that different choices of τ may sometimes produce different values of k. Recall that the number $k + 1$ gives the number of vertical lines to which a URP can be restricted without loss of information. Note also that it follows from the results of [9] that for the given values of M, τ and K_X, the URP determines the underlying zero-mean signal $x(t)$ up to a sign choice in each of the cases (2) and (4), whereas in case (1) it determines $x(t)$ up to two sign choices, and in case (3) up to one sign choice and one complex unimodular factor. Therefore it does not generally hold that a URP which is less informative on $x(t)$ will have fewer lines that still contain all its information.

Example 3 Reduction of the region of analysis for eye blink artifact detection

We present an application in EEG analysis to illustrate how redundancy in a URP can be used to reduce the search region for the detection of morphologically similar signal segments. From a digitally sampled EEG measurement signal (with sampling frequency 250 Hz) we took an excerpt of $N = 2,500$ samples with a total duration of $T = 10$ s, containing 7 eye blink artifacts. From this discrete-time measurement signal a continuous-time signal $x(t)$ was constructed, interpolating the measurement values to let $x(t)$ have a finite Fourier series. It is shown in Fig. 3a. The eye blink artifacts are clearly visible, as they occur as upward peaks having a significantly higher amplitude than the rhythmic brain activity contained in the signal. The corresponding URP was computed for the time-delay embedding parameters $M = 55$ and $\tau = 0.004$ with u and v ranging over the interval $[0, 10]$; it is displayed in Fig. 3b. It has distinctly yellow strips which mark the location of the onset of eye blinks in the signal $x(t)$. The choice of a high embedding dimension helps to locate the eye blinks, as it induces corresponding maxima in the URP, plotted in red.

For testing purposes, a second signal $y(t)$ was generated by adding Gaussian zero-mean white noise $w(t)$ with variance $\sigma^2 = 25$ to the signal $x(t)$ at the sample times, i.e. before interpolation. The high variance of the noise makes that the eye blink artifacts are no longer easily observed in the signal by mere inspection and simple thresholding does not allow their detection. This noise corrupted signal $y(t)$ is shown in Fig. 3c and its URP (for the same embedding parameters as before) is given in Fig. 3d.

The theory of this section indicates that all the information of the URP is also still contained in a limited number of vertical lines of the URP, which can be bounded above by $M + 1$. One may for instance focus attention on vertical lines which are close to each other, i.e. on a vertical strip of the URP. Note that a vertical strip which

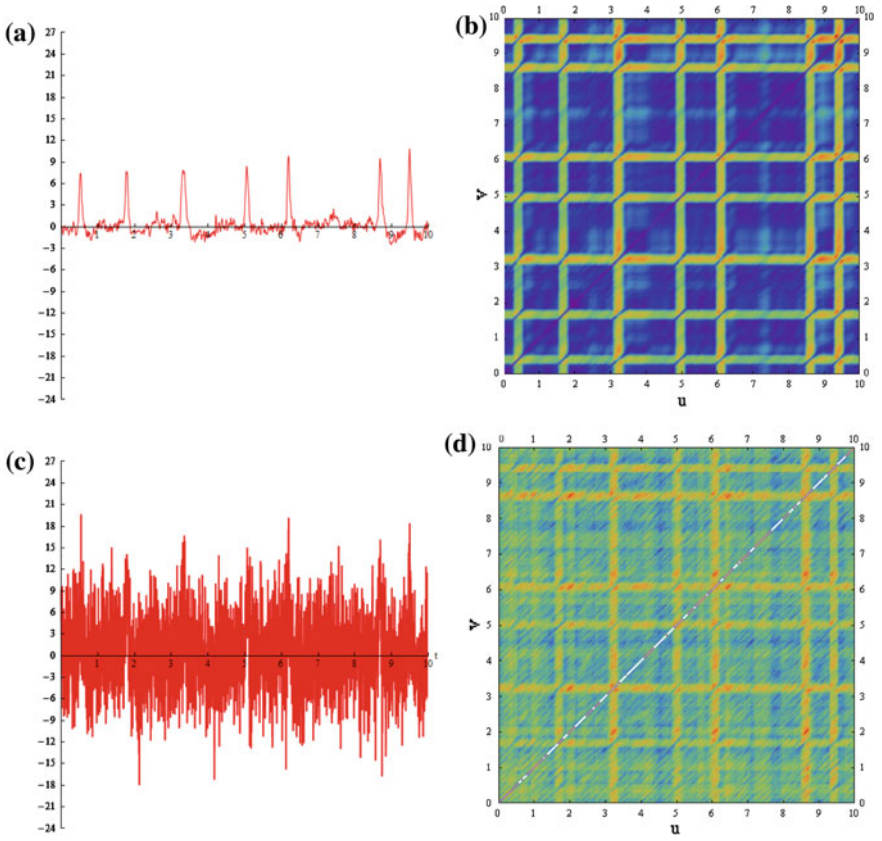

Fig. 3 **a** The interpolated EEG signal $x(t)$, containing 7 eye blink artifacts. **b** The URP of $x(t)$. **c** The noise corrupted signal $y(t) = x(t) + w(t)$ with Gaussian zero-mean white noise $w(t)$ with variance 25. **d** The URP of $y(t)$

aligns with an eye blink artifact allows one to locate the other artifacts in the URP for the clean signal $x(t)$ by searching for the local maxima in the URP. However, the same result can still be obtained for vertical strips which do not align with eye blink artifacts. In fact, for the URP of the noisy signal $y(t)$, the strips which do not align with eye blinks seem to be more promising for avoiding false positive detections (which for instance might occur near the vertical line with $u = 6.3$).

3 Distance Information Carried by Diagonals and Contour Lines

In the previous section we have demonstrated that a URP can be restricted without loss of information to just $k+1$ of its vertical (or horizontal) lines, corresponding to an affine basis of V_X. We took a geometric approach, constructing a globally rigid graph

connecting any two points $X(u)$ and $X(v)$ to all of the affine basis $\{X(t) \mid t \in \mathbb{T}_b\}$. The distance information contained in the selected vertical lines of the URP then admits the computation of $\mathrm{URP}_X(u, v)$.

In the present section we investigate the information content of different sets of lines or curves in a URP, also involving the construction of a globally rigid graph. We first study the situation for diagonals, which like vertical and horizontal lines are also used for RQA. In the discussion that follows we assume that the periodic trajectory $X(t)$ is nontrivial and sufficiently smooth (i.e. continuous or continuously differentiable with respect to t). For such $X(t)$ and its URP, a graph G and an associated framework $G(\mathcal{X})$ are now constructed in the following way.

- Choose an initial time instant $t_0 \in [0, 1)$, a time step $\Delta t > 0$, and an integer N. Let k be the dimension of the affine trajectory space V_X.
- For $n = 1, 2, \ldots, N$, define the time instants t_n by:

$$t_n = t_{n-1} + \Delta t \pmod 1. \tag{10}$$

  i.e. t_n increases linearly with n with fixed increments Δt, but the time instants are 'wrapped around' from 1 back to 0 in view of periodicity of $X(t)$.
- Let G have the nodes $\{0, 1, \ldots, N\}$ and the edge set $\{(i, j) \mid 1 \leq j - i \leq k + 1\}$.
- Let $\mathcal{X} = \{\mathcal{X}_0, \mathcal{X}_1, \ldots, \mathcal{X}_N\}$ with $\mathcal{X}_n = X(t_n)$ for $n = 0, 1, \ldots, N$ be a configuration consisting of trajectory points, and $G(\mathcal{X})$ the corresponding framework.

If N is sufficiently large, then periodicity of the sequence of time instants will occur if and only if Δt is rational. If Δt is irrational, the sequence will be dense and any two points $u, v \in [0, 1)$ will be approximated arbitrarily closely by some time instants t_i and t_j in the sequence. Now suppose that $k + 1$ consecutive points $X(t_n), \ldots, X(t_n + k)$ always constitute an affine basis for V_X. Then the framework $G(\mathcal{X})$ is globally rigid: by construction, any $k + 2$ consecutive points form a clique (i.e. a complete subgraph) which is globally rigid and fixes the position of its first (last) point relative to the last (first) $k + 1$ points. Any $k + 3$ consecutive points are then covered by two such overlapping cliques, of which the overlap consists of an affine basis of $k + 1$ consecutive points, fixing the relative positions of the first and last points and hence their distance.

The points (t_n, t_{n+1}) all lie on the diagonal line D_1 described by $v = u + \Delta t \pmod 1$ in the domain of a URP. Because of the periodic nature of the URP, we will identify opposite sides of a URP and allow curves and lines to be continued across them. Likewise, the points (t_n, t_{n+2}) all lie on the diagonal line D_2 described by $v = u + 2\Delta t \pmod 1$. Continuing in a similar fashion, we have for $\ell = 3, \ldots, k + 1$ that the points $(t_n, t_{n+\ell})$ all lie on the diagonal line D_ℓ described by $v = u + \ell \Delta t \pmod 1$. If the value of the URP is known along the diagonal lines $D_1, \ldots, D_{k+1}$, then the lengths of the bars in the framework $G(\mathcal{X})$ are all known, and by global rigidity the distance between any two points $X(t_i)$ and $X(t_j)$ can be computed. Continuity of $X(t)$ makes that such points can be used to approximate $X(u)$ and $X(v)$ arbitrarily closely. This gives the following theorem.

Theorem 2 *Let $X(t) \in \mathbb{R}^M$ be a continuous periodic trajectory with period $T = 1$. Let $k = \dim(V_X)$, where V_X is the smallest affine subspace of $\mathbb{R}^M$ containing $X(t)$ for all $t \in [0, 1)$. Let $\Delta t \in (0, 1)$ be irrational and consider the $k + 1$ diagonal lines $D_1, \ldots, D_{k+1}$ given by $D_\ell : u \mapsto v = u + \ell \Delta t \ (mod\ 1)$. If an initial point t_0 exists such that for all $n \in \mathbb{N}$, with $t_n = t_0 + n\Delta t \ (mod\ 1)$, the subset of $k + 1$ consecutive trajectory points $X(t_n), \ldots, X(t_{n+k})$ gives an affine basis for V_X, then the domain of $URP_X(u, v)$ can be restricted to the diagonals $D_1, \ldots, D_{k+1}$ without loss of information.*

This theorem strongly suggests that, generically, the information of a URP is not only contained along $k + 1$ of its vertical lines, but also along $k + 1$ suitably chosen diagonals. The remaining open issue concerns the existence of an initial time instant t_0 with the properties required by the theorem, for a suitable large class of trajectories $X(t)$.

We proceed to study the information content of $k+1$ curves in the URP, one of which is a contour line. To fix terminology, the *level set* L_d of a URP for a given value $d > 0$ is defined to consist of all the points (u, v) for which $URP_X(u, v) = d$. A level set typically consists of one or several curves which are *contour lines* of the URP; they make up the connected components of the level set L_d. Again we identify opposite sides of a URP so that contour lines can continue across them. Note that a (binary, thresholded) RP is basically obtained from a URP by determining the level set for a specified value $d = \varepsilon$. This study aims to better understand the loss of information that occurs when thresholding a URP to produce an RP.

We now construct a graph G and an associated framework $G(\mathcal{X})$ largely as before when studying diagonals, but with the following adaptations.

- We choose an additional distance value $d > 0$, but the time step Δt is no longer needed.
- For $n = 1, 2, \ldots, N$, the time instants t_n are no longer generated according to Eq. (10), but instead by:

$$t_n = \min\{\tilde{t} > t_{n-1} \mid \mathrm{URP}_X(\tilde{t} \ (\mathrm{mod}\ 1), t_{n-1}) = d\} \ (\mathrm{mod}\ 1). \tag{11}$$

  i.e. t_n is the earliest time instant after t_{n-1} for which $\|X(t_n) - X(t_{n-1})\| = d$, where time instants are 'wrapped around' from 1 back to 0 in view of periodicity of $X(t)$.

For the construction to produce a valid sequence $\{t_0, t_1, \ldots, t_N\}$, a sufficient condition that we will assume to hold is $0 < d < D/2$, where $D = \max_{u,v} \mathrm{URP}_X(u, v)$. (Continuity of the periodic trajectory $X(t)$ guarantees D to exist and to have a finite value.) As before, we again assume that any subsequence of $k + 1$ consecutive trajectory points $X(t_n), \ldots, X(t_{n+k})$ gives an affine basis of V_X. Then the graph G is again globally rigid.

We have that $\|X(t_n) - X(t_{n-1})\| = d$ for all $n = 1, 2, \ldots, N$, which shows that the corresponding points (t_{n-1}, t_n) in the domain of URP_X are all located, by construction, on the level set L_d. Equation (11) defines t_n as a function of t_{n-1},

which we denote by C_1. The graph of this function may be a single contour line for the value d, or be composed of parts of one or several contour lines of L_d. The points (t_{n-2}, t_n) with $n = 2, 3, \ldots, N$ in general do not lie on a single level set. The function which generates t_n from t_{n-1} is denoted by C_2. It is obtained by applying two steps of the recursion of Eq. (11), showing that $C_2 = C_1 \circ C_1$. When d is small and $X(t)$ continuously differentiable, which admits local linearization, this curve approximates a subset of the level set L_{2d}. This subset may consist of a single contour line, or of various parts of one or several contour lines. This depends on the curvature of the trajectory and on how nearby different sections of the trajectory can be. Likewise, the points (t_{n-3}, t_n) with $n = 3, \ldots, N$ lie on the graph of the function $C_3 = C_1 \circ C_1 \circ C_1$, which, for small d, approximates a subset of L_{3d}. Continuing in a similar fashion, we construct $k+1$ curves C_ℓ which pass through the sets of points $\{(t_{n-\ell}, t_n) \,|\, n = \ell, \ell+1, \ldots, N\}$ for $\ell = 1, 2, \ldots, k+1$, respectively, and which, for small d, approximate subsets of the level sets L_d, L_{2d}, ..., $L_{(k+1)d}$. These curves C_ℓ are characterized recursively by $C_\ell = C_1 \circ C_{\ell-1}$. They have a continuous graph if and only if C_1 is continuous.

We now sketch how, if C_1 happens to be continuous and for a well chosen value of d, the values of the URP along the curves $C_1, \ldots, C_{k+1}$ can be used to compute the distance between two points $X(u_0)$ and $X(v_0)$. Let $t_0 = u_0$ and construct the sequence of time instants $u_1, u_2, \ldots, u_N$ as described above. Then, by construction, the points $(u_n, u_{n+\ell})$ are located on the curve C_ℓ for all $n = 0, 1, \ldots, N-\ell$. Because of global rigidity of the graph G, the information in the URP along the curves $C_1, \ldots, C_{k+1}$ fixes the distance between any two points $X(u_i)$ and $X(u_j)$. For sufficiently large N, exploiting periodicity of the trajectory $X(t)$, we aim for a situation in which the sequence of time instants u_n becomes dense in the interval $[0, 1)$. Before, for the diagonals D_ℓ, this required Δt to be irrational. For the current situation this requires the distance value d to be chosen such that the sequence of time instants u_n again does not become periodic. It also requires that the range of C_1, and hence the range of each curve C_ℓ, is dense in $[0, 1)$. In this way, the time instant v_0 can be approximated arbitrarily closely by a subsequence of time points u_{n_j}. Consequently, also the value of $\mathrm{URP}_X(u_0, v_0)$ can be obtained with arbitrary precision from the values $\mathrm{URP}_X(u_0, u_{n_j})$.

If C_1 is continuous and describes a contour line then, even though this procedure has numerical drawbacks and is not advocated from a practical point of view, it strongly suggests that, for a suitably selected value of d, the information contained in the URP along the curves $C_1, \ldots, C_{k+1}$ determines $\mathrm{URP}_X(u, v)$ completely. More generally, if C_1 is discontinuous and in particular if its range is not dense in $[0, 1)$, then a similar statement holds if instead of using the curve C_1, one uses the multi-valued function of which the graph is the level set L_d. Along with this, the curves C_ℓ should then be replaced by the graphs of the multi-valued functions obtained by

composing L_d with itself multiple times. This level set L_d determines the recurrence plot $\mathrm{RP}_X^d(u, v)$. Thresholding is a lossy operation and for an RP it is well known that it contains in general less information than the URP. The above discussion makes clear that by adding the information along another k well selected curves or level sets of the URP, loss of information can be avoided.

Example 4 Information along curves in the URP

To illustrate the constructions of this section, we consider a zero-mean periodic signal $x(t)$ which is specified by

$$x(t) = 8\sin(2\pi t) + 2\cos(4\pi t + \frac{1}{5}) + \sin(6\pi t + 1). \tag{12}$$

It is shown in Fig. 4a. It has a finite power spectrum with the corresponding index set $K_X = \{-3, -2, -1, 1, 2, 3\}$. We choose the embedding parameters $M = 2$ and $\tau = \frac{1}{5}$, for which the 2-dimensional periodic trajectory $X(t)$ is given in Fig. 4b. Note that $V_X = \mathbb{R}^2$ and $k = \dim(V_X) = 2$. A contour plot of the resulting URP is shown in Fig. 4c, while the RP for the threshold value $\varepsilon = 5$ is displayed in Fig. 4d. Three specific level sets, consisting of contour lines for the URP values $d = 5$, $2d = 10$, and $3d = 15$, are presented in Fig. 4e.

In Fig. 4f the three curves C_1, C_2, and C_3 for $d = 5$ are given. These are closed curves when opposite sides of the square plot area are identified, consistent with the periodicity of $X(t)$. The curve C_1 coincides with a contour line of the URP (and also of the RP) for $d = 5$. The curves C_2 and C_3 are approximations of contour lines for the URP values $2d = 10$ and $3d = 15$, respectively. (They are not very close approximations, since d is not really small.)

Starting from an initial time $t_0 = u_0 = 0.05$, the corresponding points $X(u_n)$ generated with $d = 5$ for $n = 0, 1, \ldots, 13$ are shown on the trajectory in Fig. 4b. By definition, these are such that $\|X(u_n) - X(u_{n-1})\| = 5$ for $n = 1, \ldots, 13$. The curve C_2 in the URP captures the distances $\|X(u_n) - X(u_{n-2})\|$, while the curve C_3 captures the distances $\|X(u_n) - X(u_{n-3})\|$. The globally rigid graph G has all the edges corresponding to these distances and is also displayed in Fig. 4b. It follows that the curves C_1, C_2, and C_3 jointly carry sufficient information to compute $\mathrm{URP}_X(u_0, u_n)$ for all n. The corresponding locations in the URP are also displayed in Fig. 4f. Note that the points $X(u_{11})$, $X(u_{12})$ and $X(u_{13})$ are located on $X(t)$ in between the pairs of points $X(u_0)$ and $X(u_1)$, $X(u_1)$ and $X(u_2)$, and $X(u_2)$ and $X(u_3)$, respectively. If n is increased further, this eventually produces many more points in these intervals, which can then be used to approximate any given point $X(v)$ and the value $\mathrm{URP}_X(u_0, v)$.

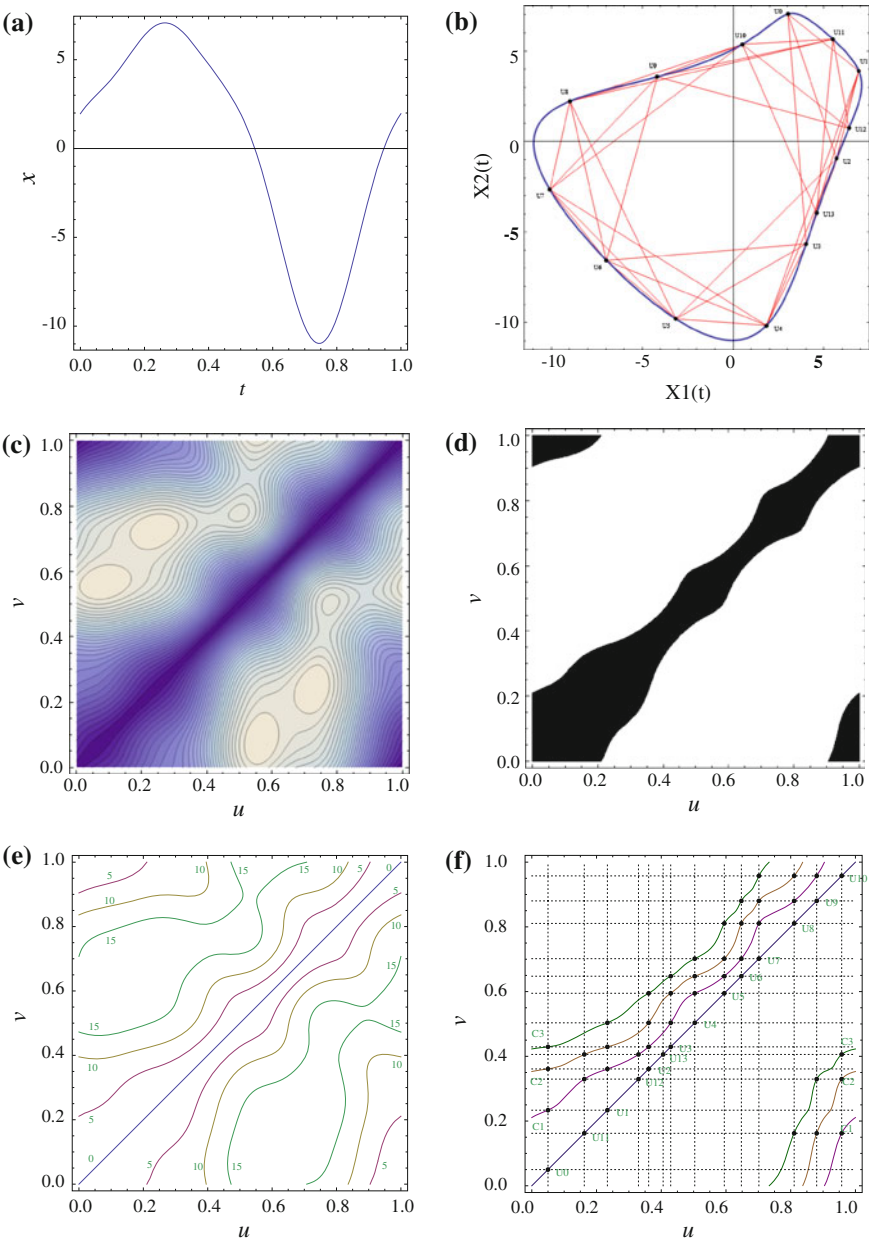

Fig. 4 **a** The zero-mean periodic signal $x(t)$ of Example 4. **b** The trajectory $X(t)$ in $\mathbb{R}^2$, the configuration of trajectory points $\mathcal{X} = \{X(u_0), \ldots, X(u_{13})\}$, and the globally rigid framework $G(\mathcal{X})$. **c** The unthresholded recurrence plot $\mathrm{URP}_X(u, v)$ for $M = 2$ and $\tau = \frac{1}{5}$. **d** The recurrence plot $\mathrm{RP}^5_X(u, v)$ for the threshold $\varepsilon = 5$. **e** The level sets (contour lines) for the values $d = 5$, $2d = 10$, $3d = 15$. **f** The curves C_1, C_2, C_3 and their points for times $t = u_0, u_1, \ldots, u_{13}$

4 Conclusions and Discussion

In Sect. 2, we used properties of rigid frameworks to explain geometrically how the information contained by a URP along a finite number of vertical lines, can be used to reconstruct the entire URP. This result holds for arbitrary trajectories $X(t)$, which need not come from a scalar signal through time-delay embedding. In Sect. 3 we presented a similar result for diagonal lines, and also for curves which coincide with or approximate contour lines. However, the proofs of those results strongly exploit periodicity of $X(t)$. The number of lines (or curves) needed to avoid loss of information in all these results is computed as $k+1$, where k equals the dimension of the space V_X. We neither claim nor conjecture that this number is minimal. In fact, especially when a continuous periodic scalar signal $x(t)$ is time-delay embedded to produce the trajectory $X(t)$, it may well be that fewer lines still contain all the information of a URP.

When a discrete-time recurrence plot is considered, the results of Sect. 2 still hold. The same goes for diagonal lines when Δt is chosen as a multiple of the sampling time which is relatively prime to the total number of measurements. The curves $C_1, \ldots, C_{k+1}$, though, are less easy to generalize to discrete-time, because they may involve time instants that are no integer multiples of the sampling time.

Regarding the information contained in a (thresholded) RP, we note that our results suggest that the information from a finite number of other curves in the URP may help to restore full information. In our opinion it does not seem likely that the choice of these curves is very critical, although convenient choices may give easier proofs. An interesting topic for further research is to investigate whether the contour lines in multi-level recurrence plots (obtained from URPs by thresholding at several levels instead of just one) may carry the full information of a URP.

In Example 3 we showed how the results of Sect. 2 can be combined with characteristics of an EEG signal to develop a novel method for artifact detection using vertical lines. Similar approaches can be investigated which involve diagonal lines or (approximate) contour plots. This theoretical study may serve as a basis to improve existing recurrence plots based methods and algorithms, and we expect it to provide new opportunities for signal analysis and feature selection.

Acknowledgments 1. This research is conducted in collaboration with and supported by BrainMarker BV, the Netherlands, in the course of its development of a decision support system for EEG based brain state analysis. 2. We want to thank an anonymous referee for his valuable comments which helped to substantially improve the paper.

Appendix

Proof of Lemma 1.
(1) For $X(t) \in V_X$ we have that $X(t) = \sum_{m=0}^{k} \alpha_m(t) X(t_m)$ in which the affine coordinates $\alpha_0(t), \alpha_1(t), \ldots, \alpha_k(t)$ add up to 1. For the translated trajectory

$\widetilde{X}(t) = X(t) - X(t_0)$ it then holds that: $\widetilde{X}(t) = \left(\sum_{m=0}^{k} \alpha_m(t) X(t_m)\right) - X(t_0) = \left(\sum_{m=0}^{k} \alpha_m(t) X(t_m)\right) - \left(\sum_{m=0}^{k} \alpha_m(t) X(t_0)\right) = \sum_{m=1}^{k} \alpha_m(t)(X(t_m) - X(t_0)) = B\alpha(t)$. This shows how the affine coordinates of $X(t)$ are related to the linear vector space coordinates of $\widetilde{X}(t)$ for the basis in the columns of B.
The matrix B has full column rank k, so the $k \times k$ Gram matrix $B^T B$ is invertible. From $\widetilde{X}(t) = B\alpha(t)$ it then follows upon premultiplication by $(B^T B)^{-1} B^T$, that $\alpha(t) = (B^T B)^{-1} B^T \widetilde{X}(t)$, which proves part (1) of the lemma.
(2) With the given definition of $A(t)$ in terms of the coordinate vector $\alpha(t)$, the right-hand side of Eq. (5) becomes: $(\alpha(u) - \alpha(v))^T B^T B \left(B^T B\right)^{-1} B^T B (\alpha(u) - \alpha(v)) = (\alpha(u) - \alpha(v))^T B^T B (\alpha(u) - \alpha(v)) = \| B (\alpha(u) - \alpha(v)) \|^2 = \| \widetilde{X}(u) - \widetilde{X}(v) \|^2$.
(3) Since $A(t) = B^T \widetilde{X}(t)$, the entry $A_m(t)$ equals the inner product $\langle \widetilde{X}(t_m), \widetilde{X}(t) \rangle$. It is well-known that an inner product between two vectors w_1 and w_2 on a real vector space can be expressed in terms of its induced norm as $\langle w_1, w_2 \rangle = \frac{1}{2}(\|w_1 + w_2\|^2 - \|w_1\|^2 - \|w_2\|^2)$. Choosing $w_1 = \widetilde{X}(t_m)$ and $w_2 = -\widetilde{X}(t)$, and noting that $\|\widetilde{X}(t)\|^2 = \mathrm{URP}_X(t, t_0)^2$, part (3) of the lemma follows.
(4) This follows from the observation that $\left(B^T B\right)_{m,n} = \langle \widetilde{X}(t_m), \widetilde{X}(t_n) \rangle = A_m(t_n)$, where m and n can be interchanged because of symmetry. □

Proof of Theorem 1.
Suppose that $(u_0, v_0) \in \mathbb{T}_a \times \mathbb{T}_a$. Then, from part (2) of Lemma 1 it follows that $\mathrm{URP}_X(u_0, v_0)$ is determined by the vectors $A(u_0)$ and $A(v_0)$, and the matrix $B^T B$. From part (3) of Lemma 1, the vector $A(u_0)$ is determined by the restriction of $\mathrm{URP}_X(u, v)$ to $\mathbb{T}_b \times \{u_0\}$. Similarly, the vector $A(v_0)$ is determined by the restriction of $\mathrm{URP}_X(u, v)$ to $\mathbb{T}_b \times \{v_0\}$. Hence, the difference $A(u_0) - A(v_0)$ is determined by the restriction of $\mathrm{URP}_X(u, v)$ to $\mathbb{T}_b \times \{u_0, v_0\}$.
From part (4) it follows that the matrix $B^T B$ is determined by the restriction of $\mathrm{URP}_X(u, v)$ to $\mathbb{T}_b \times \mathbb{T}_b$.
Together, this implies that the value of $\mathrm{URP}_X(u_0, v_0)$ is determined by the restriction of $\mathrm{URP}_X(u, v)$ to $\mathbb{T}_b \times (\mathbb{T}_b \cup \{u_0, v_0\})$. (Recall that symmetry applies to any URP.) Part (2) of the theorem now follows by letting u_0 and v_0 range over all of $\mathbb{T}_a$. Part (1) then follows by taking $\mathbb{T}_a = [0, 1)$. □

Proof of Proposition 1.
Clearly, the trajectory $X(t)$ is contained in the space spanned by the vectors T_p. The dimension k of the affine space V_x is equal, by definition, to the dimension of the linear vector space obtained as $V_X - X_0$ for any point X_0 contained in V_X. Choosing $X_0 = c_0 T_0 = c_0(1, \ldots, 1)^T$, which is contained in V_X as it is the mean of all the points for one period of the periodic trajectory $X(t)$, we therefore focus of the translated trajectory $\widetilde{X}(t) = X(t) - c_0 T_0 = \sum_{p \in \mathbb{Z} \setminus \{0\}} c_p e^{2\pi p t i} T_p$. By definition of K_X, this equals $\widetilde{X}(t) = \sum_{p \in K_X} c_p e^{2\pi p t i} T_p$.

For $M \geq 2$, two vectors T_p and T_q are equal if and only if $z^p = z^q$, which holds if and only if $(p - q)\tau$ is integer. We therefore consider the equivalence relation on K_X defined by: $p \sim q$ if and only if $(p - q)\tau \in \mathbb{Z}$. Then the equivalence classes are

characterized by the fractional parts of the numbers $p\tau$, with $p \in K_X$. We now define $R_X := \{p\tau \pmod 1 \mid p \in K_X\}$ and $L := R_X/\tau \subset \mathbb{N}$. The set L is used to index these equivalence classes. For each $\ell \in L$ the corresponding equivalence class is given by $M_\ell := \{p \in K_X \mid p\tau = \ell\tau \pmod 1\}$. With this notation the set K_X can be partitioned into its equivalence classes and we may write $\widetilde{X}(t) = \sum_{\ell \in L} \left(\sum_{p \in M_\ell} c_p e^{2\pi pti} \right) T_\ell$.

First, it is noted that: (1) M_ℓ is not empty for all $\ell \in L$; (2) $c_p \neq 0$ for all $p \in M_\ell$; (3) the functions $e^{2\pi pti}$ are all independent harmonic functions on $[0, 1]$ for all $p \in \mathbb{Z}$. This proves part (1) of the proposition, and for all $\ell \in L$ we have that $\sum_{p \in M_\ell} c_p e^{2\pi pti} \not\equiv 0$ on $[0, 1]$. Second, it is observed that any selection of $j \leq M$ vectors $\{T_{\ell_1}, \ldots, T_{\ell_j}\}$ with distinct indices $\ell_1, \ldots, \ell_j \in L$, is independent (because these vectors can be joined to form the columns of a Vandermonde matrix). Hence, it follows that $\dim(V_X) = \min\{M, |L|\}$. This proves part (2) because $r = |K_X| = |L|$.

Finally, for $M = 1$ the proposition is also easily verified to hold. □

References

1. Eckmann, J.P., Oliffson Kamphorst, S., Ruelle, D.: Recurrence plots of dynamical systems. Europhys. Lett. **4**(9), 973–977 (1987)
2. Marwan, N., Romano, M.C., Thiel, M., Kurths, J.: Recurrence plots for the analysis of complex systems. Phys. Rep. **438**(5), 237–329 (2007)
3. Webber, C.L., Zbilut, J.P.: Dynamical assessment of physiological systems and states using recurrence plot strategies. J. Appl. Physiol. **76**(2), 965–973 (1994)
4. Marwan, N.: How to avoid potential pitfalls in recurrence plot based data analysis. Int. J. Bifurcation Chaos **21**(04), 1003–1017 (2011)
5. Website on recurrence plots and cross recurrence plots. http://www.recurrence-plot.tk. Accessed online 1 Nov 2013 (2013)
6. Takens, F.: Detecting strange attractors in turbulence. In: Rand, D., Young, L. (eds.) Dynamical Systems and Turbulence. Lecture Notes in Mathematics, vol. 898, pp. 366–381. Springer, Berlin (1981)
7. Fraser, A.M., Swinney, H.L.: Independent coordinates for strange attractors from mutual information. Phys. Rev. A **33**(2), 1134–1140 (1986)
8. Kennel, M.B., Brown, R., Abarbanel, H.D.I.: Determining embedding dimension for phase-space reconstruction using a geometrical construction. Phys. Rev. A **45**(6), 3403–3411 (1992)
9. Sipers, A., Borm, P., Peeters, R.: On the unique reconstruction of a signal from its unthresholded recurrence plot. Phys. Lett. A **375**(24), 2309–2321 (2011)
10. Chen, Y., Yang, H.: Multiscale recurrence analysis of long-term nonlinear and nonstationary time series. Chaos, Solitons & Fractals **45**(7), 978–987 (2012)
11. McGuire, G., Azar, N.B., Shelhamer, M.: Recurrence matrices and the preservation of dynamical properties. Phys. Lett. A **237**(1), 43–47 (1997)
12. Hirata, Y., Horai, S., Aihara, K.: Reproduction of distance matrices and original time series from recurrence plots and their applications. Eur. Phys. J. Special Topics **164**(1), 13–22 (2008)
13. Jie, L., Shu-Ting, S., Jun-Chan, Z.: Comparison study of typical algorithms for reconstructing time series from the recurrence plot of dynamical systems. Chin. Phys. B **22**(1), 010–505 (2013)
14. Robinson, G., Thiel, M.: Recurrences determine the dynamics. Chaos **19**(2), 023–104 (2009)
15. Thiel, M., Romano, M.C., Kurths, J.: How much information is contained in a recurrence plot? Phys. Lett. A **330**(5), 343–349 (2004)
16. Birleanu, F.M., Candel, I., Ioana, C., Gervaise, C., Serbanescu, A., Serban, G.: A vector approach to transient signal processing. In: Information Science, Signal Processing and their Applications (ISSPA), 2012 11th International Conference on, pp. 1141–1146 (2012)

17. Birleanu, F.M., Ioana, C., Gervaise, C., Chanussot, J., Serbanescu, A., Serban, G.: On the recurrence plot analysis method behaviour under scaling transform. In: Statistical Signal Processing Workshop (SSP), 2011 IEEE, pp. 789–792 (2011)
18. Birleanu, F.M., Ioana, C., Serbanescu, A., Chanussot, J.: A time-distributed phase space histogram for detecting transient signals. In: Acoustics, Speech and Signal Processing (ICASSP), IEEE International Conference on 2011, pp. 3844–3847 (2011)
19. Facchini, A., Kantz, H., Tiezzi, E.: Recurrence plot analysis of nonstationary data: The understanding of curved patterns. Phys. Rev. E **72**(2), 021–915 (2005)
20. Gao, J., Cai, H.: On the structures and quantification of recurrence plots. Phys. Lett. A **270**(12), 75–87 (2000)
21. Alfakih, A.Y.: On dimensional rigidity of bar-and-joint frameworks. Discrete Appl. Math. **155**(10), 1244–1253 (2007)
22. Asimow, L., Roth, B.: The rigidity of graphs. Trans. Amer. Math. Soc. **245**, 279–289 (1978)
23. Jordán, T., Szabadka, Z.: Operations preserving the global rigidity of graphs and frameworks in the plane. Comput. Geom. **42**(67), 511–521 (2009)